Adenylate kinase 1 gene deletion disrupts muscle energetic economy despite metabolic rearrangement

Edwin Janssen, Petras P.Dzeja[1],
Frank Oerlemans, Arjan W.Simonetti[2],
Arend Heerschap[2], Arnold de Haan[3],
Paula S.Rush[4], Ronald R.Terjung[4],
Bé Wieringa[5] and Andre Terzic[1]

Departments of Cell Biology and [2]Diagnostic Radiology, University Medical Center, University of Nijmegen, [3]Institute for Fundamental and Clinical Human Movement Sciences, Vrije University Amsterdam, The Netherlands, [1]Division of Cardiovascular Diseases, Departments of Medicine, Molecular Pharmacology and Experimental Therapeutics, Mayo Clinic, Rochester, MN 55905 and [4]Biomedical Sciences College of Veterinary Medicine, University of Missouri, Columbia, MO 65211, USA

[5]Corresponding author
e-mail: b.wieringa@celbi.kun.nl

Efficient cellular energy homeostasis is a critical determinant of muscle performance, providing evolutionary advantages responsible for species survival. Phosphotransfer reactions, which couple ATP production and utilization, are thought to play a central role in this process. Here, we provide evidence that genetic disruption of AK1-catalyzed β-phosphoryl transfer in mice decreases the potential of myofibers to sustain nucleotide ratios despite up-regulation of high-energy phosphoryl flux through glycolytic, guanylate and creatine kinase phosphotransfer pathways. A maintained contractile performance of AK1-deficient muscles was associated with higher ATP turnover rate and larger amounts of ATP consumed per contraction. Metabolic stress further aggravated the energetic cost in AK1$^{-/-}$ muscles. Thus, AK1-catalyzed phosphotransfer is essential in the maintenance of cellular energetic economy, enabling skeletal muscle to perform at the lowest metabolic cost.

Keywords: adenylate kinase/creatine kinase/energy homeostasis/knockout mice/phosphoryl transfer

Introduction

Adenine nucleotides are the primary high-energy phosphoryl-carrying molecules in a living cell. Along with their energetic role, ATP, ADP and AMP are major regulators of essential cellular processes, including gene expression, ion channel gating, and receptor- or protein kinase-mediated signal transduction (Tullson and Terjung, 1991; Hardie and Carling, 1997; Dzeja and Terzic, 1998). Although the energetic and regulatory functions of adenine nucleotides are dependent on nucleotide ratios and rates of nucleotide exchange between cellular compartments (van Deursen *et al*., 1993; Steeghs *et al*., 1997; Saks *et al*., 1998; Saupe *et al*., 1998; Dzeja *et al*., 1999), the molecular mechanisms governing the dynamics of adenine nucleotide metabolism remain poorly understood.

Adenylate kinase (AK; EC 2.7.4.3), by virtue of its ability to catalyze the reaction ATP + AMP ↔ 2ADP, has been considered a key enzyme in the synthesis, equilibration and regulation of adenine nucleotides (Noda, 1973; Schulz *et al*., 1986). Through its unique property of transferring and providing for utilization both β- and γ-phosphoryls of ATP, AK doubles the energetic potential of the ATP molecule (Zeleznikar *et al*., 1990; Dzeja *et al*., 1998). By regulating ADP and AMP levels, AK renders these nucleotides active components in metabolic signaling determining the cellular response to stress (Elvir Mairena *et al*., 1996; Olson *et al*., 1996; Hardie and Carling, 1997; Dzeja and Terzic, 1998; Dzeja *et al*., 1999). Several AK isoforms have been cloned, and exhibit different levels of tissue expression with distinct intracellular distribution (Tanabe *et al*., 1993). Tissues with high energy demand, such as skeletal muscle, are particularly rich in AK1, the major enzyme isoform. AK1 is localized in the cytosol, clustered within myofibrils or bound to membranes (Wegmann *et al*., 1992; Tanabe *et al*., 1993; Elvir Mairena *et al*., 1996; Collavin *et al*., 1999). Other isoforms, such as AK2 and AK3, are less abundant in muscle and are generally confined to the mitochondrial intermembrane space or mitochondrial matrix (Noda, 1973; Nobumoto *et al*., 1998). The presence of AK in different compartments implicates this enzyme in promoting intracellular energy transfer and in communication between ATP-consuming and ATP-utilizing cellular sites (Bessman and Carpenter, 1985; Zeleznikar *et al*., 1990; Dzeja *et al*., 1998). In fact, the AK system has been found to facilitate high-energy phosphoryl transfer from mitochondria to myofibrils (Dzeja *et al*., 1999). Moreover, evidence is accumulating in support of an integrated intracellular high-energy phosphoryl transfer network comprised of AK, creatine kinase (CK) and glycolytic phosphotransfer enzymes (Wallimann *et al*., 1992; Savabi, 1994; Dzeja *et al*., 1998). Although AK appears to be essential in cellular energetics, the significance of this enzyme in maintaining intracellular energy flow has not been determined.

To obtain direct information on mechanisms regulating the economy of cellular energetics, we generated knockout mice lacking the major AK isoform, AK1. Lack of AK1 disrupted muscle energetic economy and induced remodeling in pathways for ATP production, high-energy phosphotransfer and ATP utilization, underscoring the significance of AK in sustaining efficient cellular energetics. The observed metabolic rearrangement in glycolytic, CK and guanine nucleotide phosphotransfer systems in the AK1-deficient mice demonstrates a high plasticity of muscle energetics, and may provide a mechanism for the maintenance of energetic homeostasis under metabolic stress.

Results

Cloning of the genomic AK1 gene and generation of AK1$^{-/-}$ mutant mice

By screening a genomic mouse 129/Sv phage library, several phages were isolated that contained the entire AK1 gene, including upstream and downstream flanking segments. The structural organization of the AK1 gene in these phages (Figure 1A), which spans a total of 12 kbp and comprises seven exons, has an exon–intron distribution that appears highly conserved when compared with other species, including man (Matsuura *et al.*, 1989). For disruption of the AK1 gene, a targeting vector (Figure 1A) was constructed in which the left and right arms of homology spanned 2.6 and 4.1 kbp, respectively. Exons 3–5 (encoding the ATP binding site) plus adjacent intron segments were deleted from the vector and replaced by a hygromycin B resistance cassette, inserted in antiparallel orientation. By gene targeting applied to mouse E14 embryonic stem (ES) cells (van Deursen and Wieringa, 1992; van Deursen *et al.*, 1993; Steeghs *et al.*, 1997), five cell clones with the desired genotypic modification were obtained. All ES clones had undergone correct homologous recombination events, downstream as well as upstream of the replacement mutation, as confirmed by Southern blot analysis (Figure 1B and C). Successful disruption of the AK1 gene was confirmed at the RNA level by northern blot analysis (Figure 1D), and at the protein level by zymogram analysis of protein extracts (Figure 1E–G). No residual mRNA was detected upon hybridization with an AK1 cDNA probe spanning exons 5–7, suggesting that a true null mutation was generated with respect to RNA and protein production. It is of note here that lack of AK1 in animals kept under normal housing conditions did not induce overt developmental or physiological abnormalities (not illustrated).

Absence of AK-catalyzed phosphotransfer in skeletal muscle from AK1$^{-/-}$ mice

Genetic deletion of AK1 produced loss of ^{18}O incorporation into β-phosphoryls of ATP, indicating a lack of AK-catalyzed phosphotransfer in AK1-knockout skeletal muscle (Figure 2). The percentage of β-ATP ^{18}O labeling was 4.43 ± 0.33 in wild type ($n = 6$) and 0.04 ± 0.02 in AK1-knockout ($n = 6$, $p < 0.001$; Figure 2). AK phosphotransfer flux in wild type was 4.25 ± 0.31 nmol ADP/min/mg protein or 20% of total ATP turnover in contracting (2 Hz) muscle. In AK1-knockout, AK phosphotransfer flux was 0.05 ± 0.01 nmol ADP/min/mg protein or <0.2% of total ATP turnover. Adenine nucleotide-dependent

AK activity was 3621 ± 218 nmol ATP/min/mg protein in the wild type, but only 11 ± 3 nmol ATP/min/mg protein in the AK1-knockout ($p < 0.001$). Total AK activity in the AK1-knockout muscle was diminished by 99.7% when compared with wild type. The remaining 0.3% of AK activity could be attributed to minor AK isoforms still present in AK1-knockout muscle. Thus, the AK1-knockout gastrocnemius–plantaris–soleus (GPS) muscle is characterized by the absence of AK-catalyzed β-phosphoryl transfer, which remains uncompensated by remaining AK isoforms.

Adenine nucleotide levels and metabolism in AK1-knockout skeletal muscle

AK1 has been implicated in adenine nucleotide synthesis and metabolism (Noda, 1973; Schulz *et al.*, 1986). AK1$^{-/-}$ knockout skeletal muscle demonstrated maintained ATP levels: 28.3 ± 1.5 nmol/mg protein compared with 26.4 ± 0.8 nmol/mg protein in the wild type ($n = 6$). The total sum of adenine nucleotides (ATP, ADP and AMP) was also preserved in AK1-deficient muscle: 33.9 ± 1.8 nmol/mg protein compared with 31.2 ± 0.9 nmol/mg protein for the wild type ($n = 6$). *De novo* adenine nucleotide synthesis is a rather slow process (Tullson *et al.*, 1998) and thus could be supported by minor AK isoforms present in AK1-knockout muscle. However, in non-contracting AK1$^{-/-}$ gastrocnemius muscle, the ATP/ADP ratio was higher than in the wild type: 8.8 ± 0.2 versus 8.0 ± 0.2, respectively ($p < 0.03$, $n = 5$). Moreover, in GPS muscle contracting at 2 Hz, the ATP/ADP and ADP/AMP ratios were 5.6 ± 0.2 versus 6.7 ± 0.4 ($p < 0.05$, $n = 6$), and 9.3 ± 0.8 versus 5.4 ± 0.2 ($p < 0.001$, $n = 6$), in AK1$^{-/-}$ deficient and wild type, respectively (Figure 3). This suggests that AK1-deficient muscle has a lower potential to sustain nucleotide ratios during functional load.

AK-produced AMP is metabolized to IMP by AMP deaminase (AMPD), a critical enzyme in the adenine nucleotide cycle (Tullson *et al.*, 1998). The maximal activity of AMPD was lower in AK1$^{-/-}$ gastrocnemius compared with wild type (214 ± 23 versus 330 ± 30 μmol/min/g muscle, respectively; $p < 0.02$, $n = 5$). Western blot analysis of the AK1$^{-/-}$ gastrocnemius showed a 50% reduction in the expression of the 80 kDa AMPD protein ($p < 0.01$) compared with wild type (not illustrated). Thus, although adenine nucleotide levels are maintained in AK1-deficient muscle, the dynamics of adenine nucleotide metabolism catalyzed by nucleotide metabolizing and/or phosphotransfer enzymes may be altered upon deletion of AK1.

Fig. 1. (**A**) Targeted mutagenesis of AK1 with wild-type (top) and mutant (bottom) AK1 genes shown after homologous recombination. Exons: shaded or black; introns or extragenic regions: white. In the targeting vector (middle), a selectable HygroB cassette replaces the 5.5 kb *Bam*HI–*Hin*dIII gene fragment (exons 3–5) that encodes the ATP-binding domain of AK1. A HSV-tk cassette was fused to the right arm of homology to facilitate selection of properly targeted ES clones. Lengths of restriction fragments (arrowed lines) from wild-type and mutant alleles are indicated. (**B** and **C**) Southern blot of genomic DNAs from wild-type and mutated E14 ES clones. DNAs were cleaved with *Kpn*I–*Xho*I or *Bam*HI restriction enzymes, resolved by agar gel electrophoresis, and blot-analyzed by hybridization with probes (indicated in A) that discriminate between recombination events at the 3′- (B) and 5′- (C) segments of homology. Diagnostic *Kpn*I–*Xho*I digestion yields 11.5 and 5.6 kb fragments, whereas *Bam*HI digestion results in 4 and 7 kb fragments for wild-type and mutant alleles. (**D**) Northern blot analysis of RNAs from wild-type and AK1$^{-/-}$ tissues. Blots with equivalent amounts of total RNA (10 μg) from skeletal muscle (SK), heart (H) and brain (B) probed with AK1 cDNA. Note the absence of AK1 mRNA in homozygous mutants. (**E**, **F** and **G**) Zymogram analysis of homogenates from brain (B), heart (H) and gastrocnemius (G)–plantaris (P)–soleus (S) muscle of wild-type, AK1$^{-/-}$ (homozygous) and AK1$^{+/-}$ (heterozygous) mice. AK1 and CK isoenzymes were separated by agarose gel electrophoresis under native conditions and their migration positions revealed by activity staining. Note the complete absence of staining at the AK1 position for AK1-deficient mice.
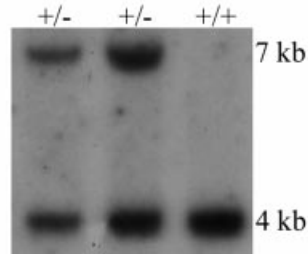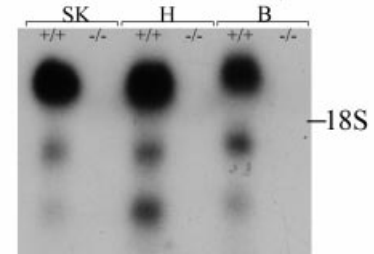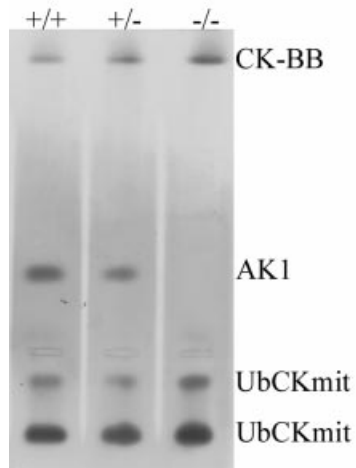
A AK1 targeting strategy
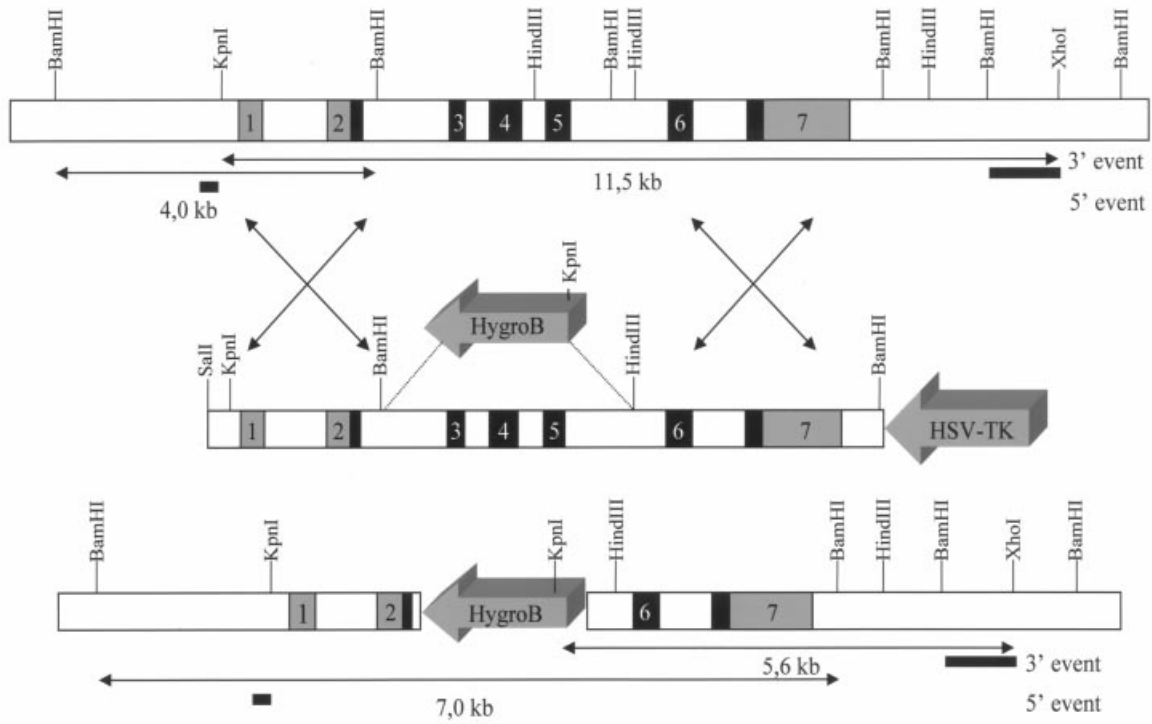
B 3'-event
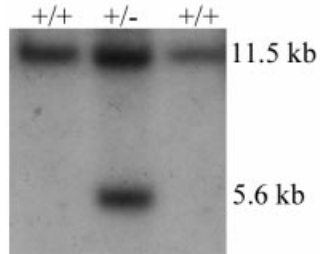
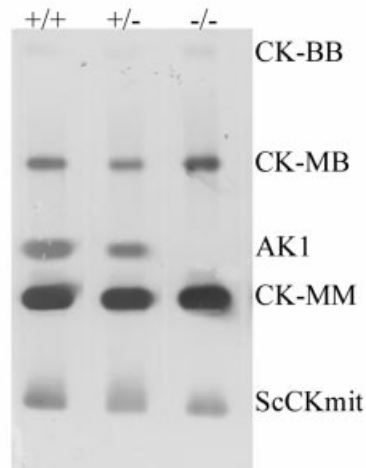**C** 5'-event
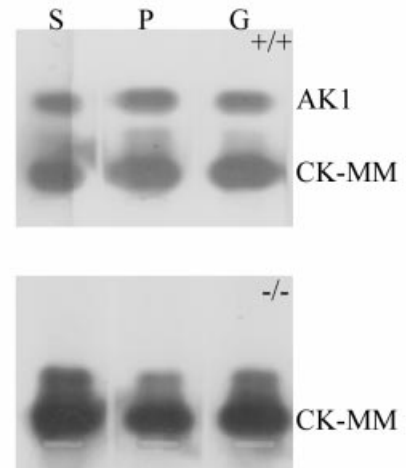

D Northern blot analysis

E Brain
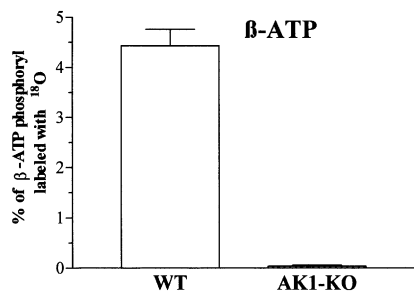

F Heart

G GPS-muscles

Fig. 2. Absence of AK phosphotransfer in AK1-knockout skeletal muscle. β-ATP phosphoryl oxygens replaced with ^{18}O, as an indicator of AK-catalyzed phosphotransfer, in wild-type (WT; $n = 6$) and AK1-knockout (AK1-KO; $n = 6$) GPS muscle.
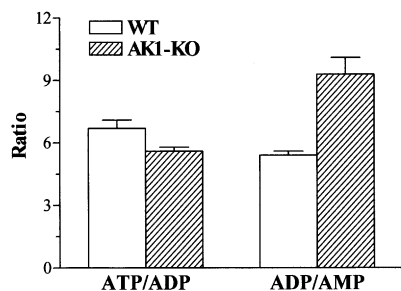

Fig. 3. Adenine nucleotide ratios in AK1-knockout skeletal muscle. ATP/ADP and ADP/AMP ratios measured in wild-type ($n = 6$) and AK1-knockout ($n = 6$) GPS muscle paced for 3 min at 2 Hz.

Creatine kinase in AK1-knockout skeletal muscle

Along with AK, CK provides a major pathway for regulation of nucleotide ratios and energy transfer (Wallimann *et al.*, 1992; van Deursen *et al.*, 1993; Veksler *et al.*, 1995; Dzeja *et al.*, 2000). Wild-type and AK1-deficient GPS muscle extracts contained essentially equal levels of creatine phosphate (CrP): 50.4 ± 3.0 ($n = 6$) and 47.8 ± 3.2 ($n = 6$) nmol CrP/mg protein, respectively. Moreover, *in vivo* changes in CrP levels, measured by ^{31}P-NMR spectroscopy, during metabolic transitions exhibited similar profiles in wild-type and AK1$^{-/-}$ hind leg muscles (Figure 4A). However, in AK1-knockout GPS, the percentage of CrP ^{18}O labeling was 21.9 ± 1.7 ($n = 6$) compared with 15.8 ± 1.3 ($n = 6$) in the wild type ($p < 0.05$; Figure 4B), indicating increased turnover of substrates in the CK-catalyzed reaction. This translated into a moderate increase in net CK-catalyzed phosphotransfer flux (13.9 ± 1.4 and 16.5 ± 1.1 nmol CrP/min/mg protein in wild type and AK1-knockout, respectively). Thus, while CrP is maintained at wild-type level in the AK1-knockout skeletal muscle, the relative CK-catalyzed CrP turnover appears increased upon deletion of AK1.

Glycolytic phosphotransfer and glycolytic intermediates in AK1-knockout muscle

AK phosphotransfer is coupled to glycolysis and regulates the activity of ATP- and AMP-sensitive glycolytic enzymes (Ottaway and Mowbray, 1977; Zeleznikar *et al.*, 1995). In turn, glycolysis also serves a high-energy phosphoryl transfer function in parallel with AK and CK (Dzeja *et al.*, 1998, 2000). Here, deletion of AK1 affected
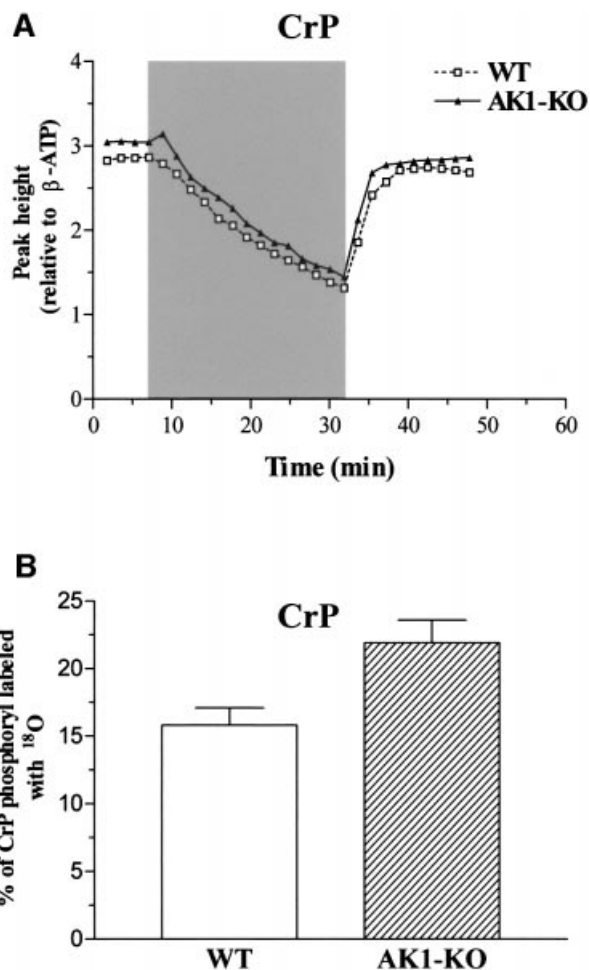

Fig. 4. Creatine phosphate levels and CK phosphotransfer in AK1-knockout skeletal muscle. (**A**) Levels of CrP in wild-type and AK1$^{-/-}$ mice, analyzed by ^{31}P-NMR and expressed as resonance peak heights normalized to the mean value of the β-ATP intensity of the first four spectra. Series were recorded every 108 s (90° pulses) before, during and after ischemia of the lower hind limb muscles in wild-type (dashed line, open squares) and AK1-deficient (solid line, closed triangles) mice. After four reference spectra, an ischemic period of 25 min (shaded area) was introduced succeeded by a recovery of 16 min. (**B**) Increased CK-catalyzed CrP turnover in AK1-knockout muscle. Percentage of CrP-phosphoryl oxygens replaced with ^{18}O, as an indicator of CK-catalyzed phosphotransfer, in wild-type ($n = 6$) and AK1-knockout ($n = 6$) GPS muscle, determined by mass spectrometry.

glycolytic phosphotransfer, as well as levels of glycolytic intermediates. Glycolytic phosphotransfer was assessed by hexokinase-catalyzed incorporation of ^{18}O into glucose-6-phosphate (G-6-P), which increased from 8.4 ± 0.3 ($n = 6$) in wild type to 11.2 ± 0.6 ($n = 6$) in AK1-knockout muscle ($p < 0.05$), at a labeling rate of 0.66 ± 0.03 and 0.151 ± 0.05 nmol/min/mg protein $\times$ 10^{-1} ($p < 0.01$; Figure 5A), respectively. The estimated net glycolytic flux was increased from 1.31 ± 0.06 to 3.00 ± 0.09 nmol G-6-P/min/mg protein in wild-type and AK1-knockout muscle, respectively ($p < 0.01$). Increased glycolytic flux was accompanied by higher muscle levels of G-6-P (7.8 ± 1.0 and 13.6 ± 1.6 nmol/mg protein in wild type and AK1-knockout; $n = 6$, $p < 0.001$) and lactate (8.3 ± 0.7 and 12.6 ± 2.1 nmol/mg protein in wild type and AK1-knockout; $n = 6$, $p < 0.001$). Alterations in glycolytic metabolism were

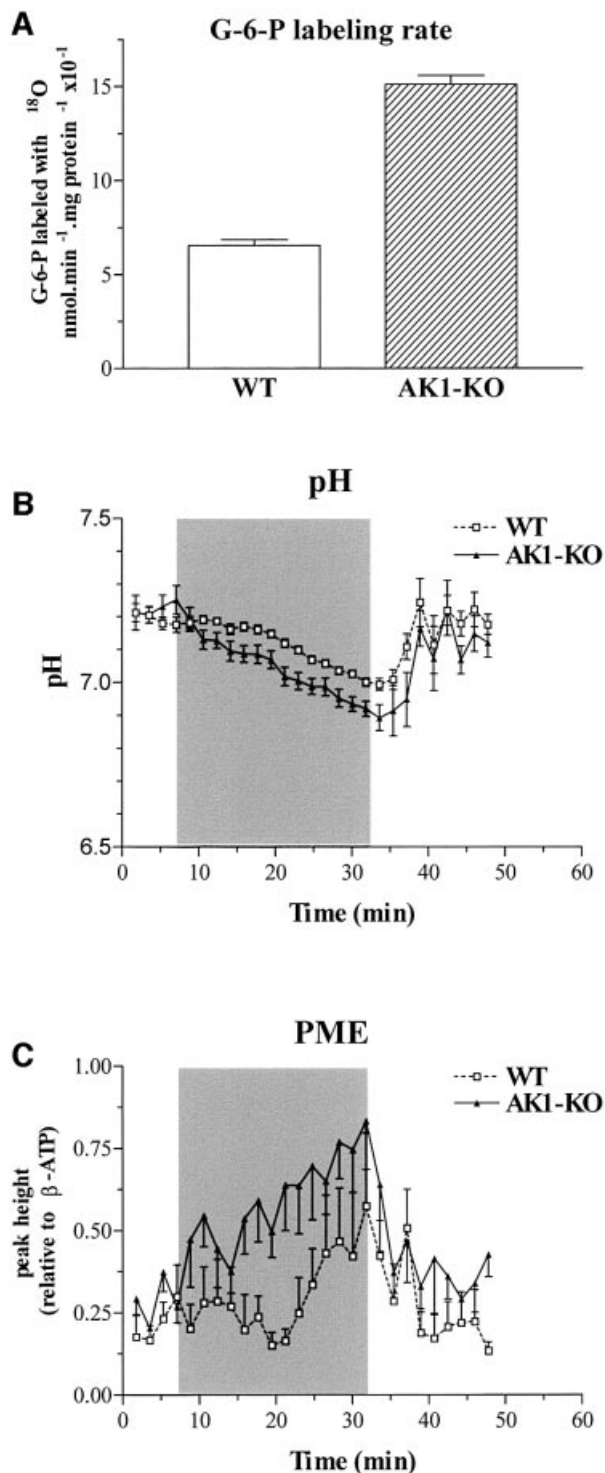**Fig. 5.** (**A**) Increased hexokinase-catalyzed G-6-P turnover in AK1-knockout muscle. Glucose-6-phosphate phosphoryl oxygens replaced with ^{18}O, as an indicator of glycolytic phosphotransfer, in wild-type ($n = 6$) and AK1-knockout ($n = 6$) GPS muscle. (**B** and **C**) Intracellular pH (B) and PME levels (C) in wild-type (WT) and AK1$^{-/-}$ mice, analyzed by ^{31}P-NMR and expressed in pH units or as resonance peak heights normalized to the mean value of the β-ATP intensity of the first four spectra. Series were recorded before, during and after ischemia of the lower hind limb muscles in wild-type (dashed line, open squares) and AK1-deficient (solid line, closed triangles) mice. After four reference spectra, an ischemic period of 25 min was introduced succeeded by a recovery of 16 min. Note a faster pH decrease and increased PME levels during the ischemic period in AK1$^{-/-}$ compared with wild-type mice.

further assessed *in vivo* by monitoring phosphomonoester (PME)-containing glycolytic intermediates and intracellular pH by ^{31}P-NMR spectroscopy. Ischemia induced a faster muscle acidification in AK1-mutant mice (Figure 5B), suggesting that the block in β-phosphoryl exchange between ADP and ATP is associated with accelerated anaerobic glycolysis and production of lactate. Moreover, the increase in PME levels was significantly more pronounced in AK1-deficient mutant mice (Figure 5C). This increase in the intracellular concentration of glycolytic intermediates, along with increased G-6-P turnover, indicates elevated glycolytic metabolism in AK1-knockout muscle.

Guanine nucleotide metabolism in AK1-knockout skeletal muscle

Adenine nucleotide metabolism is coupled to guanine nucleotide metabolism through the nucleoside diphosphate kinase (NDPK)-catalyzed phosphotransfer (Ray and Mathews, 1992). There is an important link between GTP production by substrate level phosphorylation in the Krebs cycle and ATP production in mitochondria. AK1-deficient muscle had a 50% higher intracellular GTP concentration compared with wild type, 0.75 ± 0.06 versus 0.43 ± 0.02 nmol/mg protein, respectively ($p < 0.001$, $n = 6$). Also, the GDP concentration was 17% higher in AK1$^{-/-}$ muscle compared with wild type: 0.20 ± 0.02 and 0.16 ± 0.004 nmol/mg protein, respectively ($p < 0.03$, $n = 6$). This resulted in higher muscle levels of guanine nucleotides (GTP plus GDP) in AK1$^{-/-}$ compared with wild type: 0.95 ± 0.07 versus 0.59 ± 0.02 nmol/mg protein, respectively. Also, the GTP/GDP ratio was elevated in AK1-knockout muscle compared with wild type: 3.7 ± 0.2 versus 2.7 ± 0.1, respectively ($p < 0.003$, $n = 6$; Figure 6A). Concomitantly, the ATP/GTP ratio was lower in AK1$^{-/-}$ muscle compared with wild type (38 ± 1 and 61 ± 2; $p < 0.001$, $n = 6$), indicating increased guanine nucleotide contribution to muscle energetics (Figure 6A). The NDPK activity, however, was unaltered in AK1$^{-/-}$ gastrocnemius [$19.9 \pm 1.5 \times 10^3$ relative light units (RLU)/min/mg protein; $n = 3$] compared with wild type ($21.4 \pm 1.7 \times 10^3$ RLU/min/mg protein; $n = 3$). To assess the dynamics of guanine nucleotide metabolism, the rates of [^{18}O]phosphoryl labeling of γ- and β-GTP/GDP were determined (Figure 6B). In AK1$^{-/-}$ GPS, the percentage of γ-GTP ^{18}O labeling was 26.4 ± 1.6 ($n = 6$), significantly higher than the 18.5 ± 0.5 ($n = 6$) measured in the wild type ($p < 0.05$; Figure 6B). Such an increase in γ-GTP turnover indicates that phosphoryl flux through enzymes catalyzing GTP production, such as succinyl-CoA synthase of the Krebs cycle and/or NDPK, is elevated following deletion of the AK1 gene. NAD$^+$ levels were significantly higher in freshly isolated AK1$^{-/-}$ muscle ($n = 5$) compared with wild type ($n = 5$), 3.4 ± 0.2 versus 2.8 ± 0.6 nmol/mg protein, respectively ($p < 0.02$). Moreover, the NAD$^+$/NADH ratio was higher in *in vitro* incubated AK1-deficient muscle, 1.1 ± 0.1 versus 0.7 ± 0.1 for the wild type ($p < 0.01$; $n = 6$), suggesting elevated aerobic Krebs cycle metabolism. Guanylate kinase, the AK analog in guanine nucleotide metabolism, catalyzes β-GTP/GDP turnover, providing energy from β-phosphoryls. The percentage of combined β-GTP/GDP ^{18}O labeling was
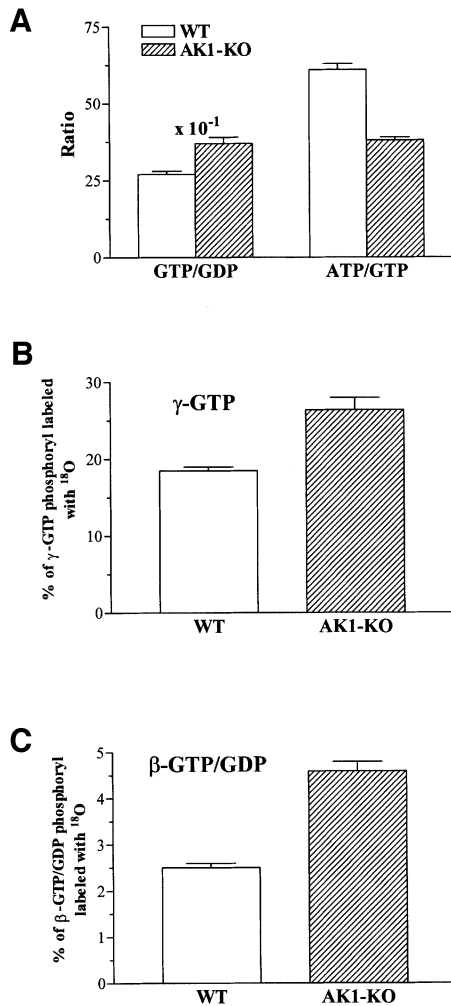
Fig. 6. Guanine nucleotide metabolism in AK1-knockout skeletal muscle. (**A**) The GTP/GDP and ATP/GTP ratios were measured in wild-type ($n = 6$) and AK1-knockout ($n = 6$) GPS muscle paced for 3 min at 2 Hz. (**B**) Increased γ-GTP phosphate turnover in AK1-knockout skeletal muscle. Percentage of γ-GTP phosphoryl oxygens replaced with ^{18}O, as an indicator of enzyme activity catalyzing GTP production, in wild-type ($n = 6$) and AK1-knockout ($n = 6$) GPS muscle. (**C**) Increased guanylate kinase-catalyzed phosphotransfer in AK1-knockout skeletal muscle. Percentage of β-GTP/GDP phosphoryl oxygens replaced with ^{18}O, as an indicator of guanylate kinase phosphotransfer, in wild-type ($n = 6$) and AK1-knockout ($n = 6$) GPS muscle.

Table I. Contractile properties of medial gastrocnemius muscles from wild-type and AK1$^{-/-}$ mice

	Control ($n = 11$)	AK1$^{-/-}$ ($n = 9$)
Twitch force (N)	0.29 ± 0.06	0.30 ± 0.07
Tetanic force (N)	1.49 ± 0.23	1.47 ± 0.32
Tetanic/twitch ratio	5.10 ± 0.94	4.78 ± 0.94
Maximal rate of force rise (%F_{max}/ms)	3.32 ± 0.69	3.54 ± 0.79
Half-relaxation time (ms)	8.4 ± 2.1	8.7 ± 2.1
Maximal shortening velocity (mm/s)	97.2 ± 1.8 ($n = 5$)	95.6 ± 18.5 ($n = 5$)
Fatigue index (%)	68.3 ± 6.6 ($n = 7$)	67.8 ± 10.0 ($n = 8$)

Data are mean $\pm$ SD for the number (n) of muscles indicated. Fatigue index: force at the end of exercise as a percentage of initial force.

has been considered an important enzyme in maintaining cellular energetic economy (Noda, 1973; Dzeja *et al.*, 1998). To assess whether AK1 gene deletion affected muscle energetic efficiency, muscle performance and ATP turnover rate were determined. AK1-deficient gastrocnemius had an isometric (twitch and tetanic) force production equivalent to that of the wild type (Table I). Also, muscle speed was not different between groups, as indicated by a similar maximal rate of force development, half-relaxation time and maximal shortening velocity (Table I). Repeated isometric contractions resulted in a similar decrease in the rate and amplitude of force generation in wild-type and mutant muscle (Table I). Thus, the overall contractile performance of an AK1-deficient muscle appears rather normal. However, γ-ATP ^{18}O labeling, reflecting muscle energy transduction rate, was significantly increased from $14.1 \pm 0.9\%$ ($n = 6$) in the wild-type to $18.4 \pm 0.5\%$ in AK1-mutant muscle ($n = 6$, $p <0.002$; Figure 7A). Furthermore, the total cellular ATP turnover, determined from ^{18}O incorporation into major high-energy phosphoryls including γ/β-ATP, CrP, inorganic phosphate, G-6-P and γ/β-GTP/GDP, was significantly increased from 21.6 ± 0.9 nmol/min/mg protein in wild-type ($n = 6$) to 26.3 ± 1.2 nmol/min/mg protein in AK1-knockout ($n = 6$) GPS, respectively ($p <0.02$; Figure 7B). Thus, the overall ATP production and utilization was elevated in AK1-knockout muscle. This translates into an increased ATP consumption per contraction from 180 ± 2 pmol ATP/mg protein in the wild-type to 219 ± 1 pmol ATP/mg protein in AK1-knockout muscles contracting at 2 Hz ($p <0.02$, $n = 6$). Such a rise in the energetic cost of contraction, by 22%, indicates reduced efficiency of cellular energetics in the absence of AK1-catalyzed phosphotransfer.

Aberrant redistribution of phosphotransfer flux and increased energy expenditure in AK1-knockout muscle during hypoxic stress

Metabolic stress induces redistribution of phosphotransfer in skeletal muscle (Zeleznikar *et al.*, 1995). AK function is believed to increase under stress to regenerate ATP and maintain muscle energetic efficiency (Dzeja *et al.*, 1996, 1999). Here, the contribution of AK-mediated phosphotransfer to total cellular ATP turnover increased from 20 ± 2 to $52 \pm 5\%$ in response to hypoxia (2 mM KCN treatment) in wild-type GPS (Figure 8A). In AK1-knock-

2.5 ± 0.1 ($n = 6$) and 4.6 ± 0.2 ($n = 6$) in wild-type and AK1-knockout GPS, respectively (p <0.001; Figure 6C). This indicates that guanylate kinase-catalyzed phosphotransfer is up-regulated in the AK1-knockout muscle. Thus, production and utilization of guanine nucleotides are increased following disruption of AK1-catalyzed phosphotransfer.

Reduced energetic efficiency of contractile performance in AK1-knockout muscle

During evolution, muscles have developed an efficient energy transduction, transfer and utilization system in order to consume a minimum amount of ATP per contraction (Mommaerts, 1969; Koretsky, 1995; Gibbs and Barclay, 1998). AK, by its ability to transfer and provide the energy of both β- and γ-phosphoryls of ATP,
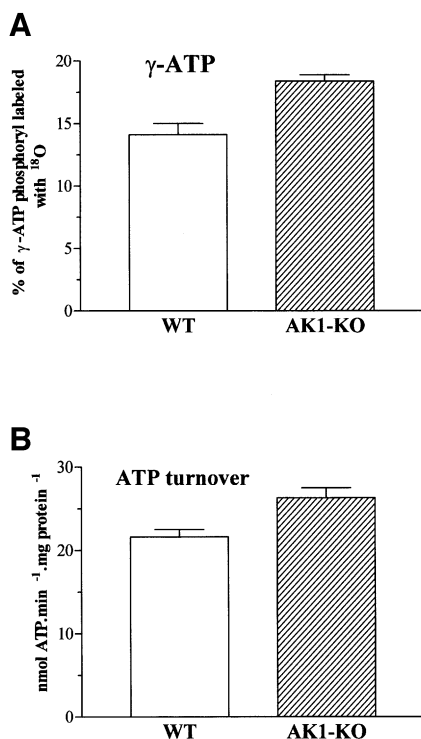
A

B

Fig. 7. Increased ATP turnover in AK1-knockout skeletal muscle. (**A**) Increased γ-ATP phosphate turnover in AK1-knockout GPS. Percentage of γ-ATP phosphoryl oxygens replaced with ^{18}O, as an indicator of ATP synthesis rate, in wild-type ($n = 6$) and AK1-knockout ($n = 6$) GPS muscle. (**B**) Increased ATP turnover in AK1-knockout skeletal muscle. Total ATP turnover, obtained from [18]O incorporation into major high-energy phosphoryls, in wild-type ($n = 6$) and AK1-knockout ($n = 6$) GPS muscle.

out muscle, AK phosphotransfer was modestly increased during hypoxia and contributed $2 \pm 1\%$ to total cellular ATP turnover (Figure 8A). With hypoxia, the contribution of CK-catalyzed phosphotransfer to intracellular energetics decreased from 64 ± 7 to $34 \pm 4\%$ in wild-type, and from 63 ± 5 to $47 \pm 4\%$ in AK1-knockout GPS (Figure 8B). Thus, wild-type GPS responds to hypoxic stress by a decrease in CK-mediated phosphotransfer associated with increased AK flux. Deletion of AK1 produces aberrant redistribution of phosphotransfer flux in hypoxic muscle, with a blunted AK response and an apparently higher contribution of CK. In wild-type skeletal muscle, the sum of AK- and CK-catalyzed phosphotransfers was essentially not changed in normoxia versus hypoxia, at 84 ± 7 and $86 \pm 4\%$ of total cellular ATP turnover, respectively (Figure 8C). However, in AK1-knockout GPS, the contribution of AK- and CK-catalyzed phosphotransfer to total ATP turnover was significantly lower than in normoxic wild-type muscle ($63 \pm 5\%$; $p <0.001$, $n = 6$), and was even further reduced under hypoxia ($49 \pm 5\%$; $p <0.001$; Figure 8C). This aberrant redistribution of phosphotransfer in AK1^{-/-} muscle translated into a more pronounced difference in total ATP turnover compared with the wild type: 22.0 ± 1.2 versus 16.8 ± 1.2 nmol/min/mg protein respectively ($p <0.02$, $n = 6$; Figure 8D). Thus, in response to hypoxia, in the wild-type muscle total ATP turnover was reduced by 19%, while in the AK1-knockout the reduction was only 10%.

Therefore, under hypoxia, the AK1-deficient muscle had a higher energy expenditure, by 31%, compared with normal muscle.

Discussion

Efficient cellular energetics is a critical determinant of muscle performance and thus an evolutionary necessity for species survival (Mommaerts, 1969; Gibbs and Barclay, 1998). Here, we provide first evidence that disruption of AK-catalyzed phosphotransfer by gene deletion leads to overt reduction in energetic efficiency of contractile performance associated with metabolic remodeling in glycolytic, CK and guanine nucleotide phosphotransfer systems. Thus, phosphotransfer reactions are an integral component of cellular energetics required for nucleotide homeostasis, optimal high-energy phosphoryl transfer and efficient ATP utilization.

Although the molecular structure and kinetic properties of the AK protein have been established (Schulz et al., 1986; Yan and Tsai, 1999), the biological significance of AK catalysis in a living cell has remained poorly understood. Here, deletion of AK1 was associated with a dramatic reduction in total muscle AK activity and lack of β-phosphoryl turnover, providing definite evidence that β-phosphoryl transfer is an exclusive property of AK catalysis that cannot be supported by other phosphotransfer reactions.

Throughout evolution, AK has been highly conserved and implicated in *de novo* adenine nucleotide synthesis and equilibration (Noda, 1973). In yeast, absence of mitochondrial AK activity compromises export of ATP from mitochondria (Bandlow et al., 1988), and generalized AK mutation can be lethal due to uncompensated disruptions in β-phosphoryl energetics and adenine nucleotide synthesis (Konrad, 1993). Here, in AK1-knockout muscle, ATP and total adenine nucleotide levels were rather preserved. Thus, the marginal AK-like activity that remains in AK1-knockout muscle is probably sufficient to support adenine nucleotide synthesis (Tullson et al., 1998). However, AK1-deficient muscle was unable to sustain ATP/ADP and ADP/AMP ratios, underscoring the importance of AK in regulating adenine nucleotide metabolism.

Through NDPK and guanylate kinase, adenine nucleotide metabolism is coupled to guanine nucleotide metabolism, which in turn serves a critical role in signal transduction (Ray and Mathews, 1992). In fact, metabolic consequences induced by NDPK deficiency can be compensated in part through AK (Lu and Inouye, 1996). Although NDPK activity was not notably changed, guanylate levels as well as guanine nucleotide β- and γ-phosphoryl turnover were significantly increased in AK1^{-/-} muscle. This increase in guanine nucleotide turnover could compensate for ~10% of lost adenine nucleotide β-turnover, indicating that metabolic flux through guanine nucleotide-dependent Krebs cycle reactions and guanylate kinase are altered following deletion of the AK1 gene. In fact, increased [γ-^{18}O]GTP labeling in AK1-knockout muscle was associated with increased activity of succinyl CoA synthetase, a Krebs cycle enzyme that couples cleavage of succinyl CoA to phosphorylation of GDP and contributes to labeling at the γ-phosphoryl
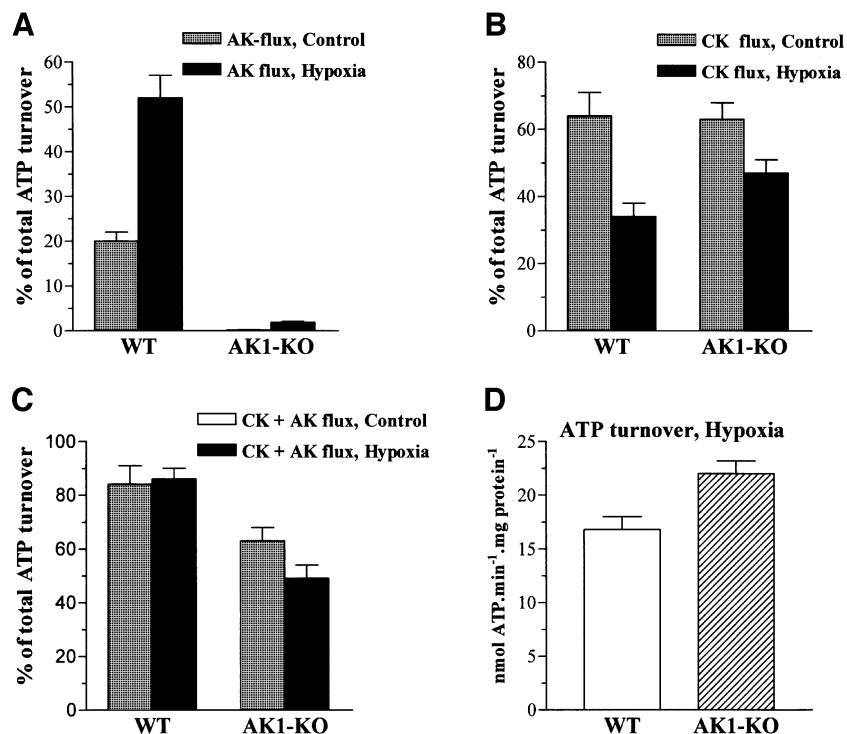
Fig. 8. Aberrant redistribution of phosphotransfer flux in AK1-knockout skeletal muscle in response to hypoxia. (**A**) Hypoxia markedly elevates AK-catalyzed flux in wild-type, but not in AK1-knockout GPS. AK-catalyzed phosphotransfer, expressed as a percentage of total cellular ATP turnover, in wild-type ($n = 6$) and AK1-knockout ($n = 6$) GPS muscle. (**B**) Increased contribution of CK-catalyzed phosphotransfer in hypoxic AK1-deficient compared with hypoxic wild-type GPS. Creatine kinase-catalyzed phosphotransfer, expressed as a percentage of total ATP turnover, in wild-type ($n = 6$) and AK1-knockout ($n = 6$) GPS muscle. (**C**) Contribution of combined AK- and CK-catalyzed phosphotransfer to cellular ATP turnover is reduced in normoxic and hypoxic AK1-knockout GPS. The sum of AK- and CK-catalyzed phosphotransfer is expressed as a percentage of total ATP turnover measured by the [^{18}O]phosphoryl labeling technique. (**D**) ATP turnover rates in wild-type and AK1-knockout GPS under hypoxia. Hypoxia was induced by KCN (2 mM), an inhibitor of mitochondrial respiration.

position in GTP (Zeleznikar and Goldberg, 1991). Also, altered mitochondrial NAD$^+$/NADH ratios suggest elevated Krebs cycle activity and increased mitochondrial involvement in AK1$^{-/-}$ muscle. Electron microscopy-ultrastructural analysis of fast-twitch fibers confirmed that these metabolic changes are paralleled by an increase in mitochondrial volume (not shown). Taken together, the observed increase in steady-state levels of guanine nucleotides and their metabolic dynamics upon disruption of adenine nucleotide homeostasis suggest an increased contribution of guanine nucleotides in AK1-knockout muscle.

In many cell types, AK-catalyzed phosphotransfer is interrelated with CK and glycolytic phosphotransfer systems (Savabi, 1994; Dzeja et al., 1998). In insulin-secreting pancreatic β-cells, increased glycolytic and CK flux, which occurs in response to elevated extracellular glucose, results in suppression of AK-catalyzed phosphotransfer (Olson et al., 1996; Dzeja and Terzic, 1998). Conversely, in skeletal muscle, inhibition of CK and/or glycolysis results in a marked increase in AK-catalyzed phosphotransfer (Dzeja et al., 1996). Here, deletion of AK1 induced adaptive changes in CK-catalyzed phosphotransfer, and up-regulation of high-energy phosphoryl flux through glycolytic metabolism. Specifically, the glycolytic flux rate more than doubled and was accompanied by a similar increase in the concentrations of glycolytic intermediates, such as G-6-P and lactate. Similarly, levels of

PME compounds (glycerol phosphate, G-1-P and G-6-P), measured *in vivo* in ischemic AK1$^{-/-}$ muscle, were twice as high as in the wild type, and were accompanied by faster accumulation of lactate and a faster decrease in intracellular pH. Although CrP levels were maintained, CK-catalyzed phosphotransfer was moderately increased in AK1$^{-/-}$ muscle compared with the wild type. Thus, the AK1-knockout muscle adapts to the lack of AK1-catalyzed phosphotransfer through up-regulation of glycolytic, along with CK and guanine nucleotide phosphotransfer systems.

This is in accord with previous studies with CK-knockout mice that also indicate a high plasticity of muscle energetic systems in adapting to genetic disruption of an energy supply pathway (van Deursen et al., 1993; Veksler et al., 1995; Dzeja et al., 1996; Steeghs et al., 1998). However, despite metabolic and cyto-architectural adaptation, deletion of the M-CK and/or ScCKmit CK isoforms resulted in an abnormal muscle contractile response, intracellular Ca^{2+} handling and mitochondrial respiration (van Deursen et al., 1993; Kay et al., 2000). Moreover, in heart muscle, deletion of CK genes reduced the ability to sustain adenine nucleotide ratios, and rendered cardiac work more 'energetically costly' in terms of high-energy phosphate use and decreases in free energy released from ATP hydrolysis (Saupe et al., 1998). Here, we demonstrate that AK1-deficient muscles exhibit a higher rate of [^{18}O-γ]phosphoryl labeling and total ATP

turnover. As the overall level of phosphoryl-containing metabolites was not significantly changed upon deletion of AK1, this indicates that the energetic efficiency of AK1-knockout muscle is lower than that of wild type.

AK1-deficient muscles did not exhibit any apparent deviation in contractile and fatigue performance compared with control muscle, suggesting that the same work output can be generated in both muscles. However, the AK1-knockout muscle did consume a larger amount of ATP per contraction, indicating lower energetic efficiency of muscle performance following AK1 deletion. Metabolic stress, which is associated with aberrant redistribution of phosphotransfer flux, further aggravated the energetic cost in an AK-deficient muscle, providing evidence for the crucial role of AK in optimal cellular energy allocation.

In conclusion, loss of AK-supported β-phosphoryl energetics disrupts adenine and guanine nucleotide home-ostasis and associated metabolic circuits (i.e. the AMPD reaction), and results in redistribution of energy flow through alternative glycolytic and CK phosphotransfer systems. Such metabolic plasticity of myocytes provides an apparent compensatory potential that limits cellular energetic failure and preserves muscle contractile per-formance. However, intracellular metabolic rearrange-ment is not sufficient to sustain energetic economy in AK1-deficient muscle, in particular under metabolic stress, suggesting a specific energetic function for AK. Thus, this study provides new evidence that phospho-transfer reactions in general, and adenylate kinase in particular, are essential for cellular energetic economy, enabling skeletal muscle to perform with high thermo-dynamic efficiency under physiological and pathophysio-logical conditions.

Materials and methods

AK1 targeting vector
Genomic DNA fragments of the AK1 gene were obtained by screening an EMBL3 phage library of partially digested genomic DNA of the mouse strain 129/Sv using rat AK1 cDNA spanning exons 5–7 as a probe (provided by Dr N.D.Goldberg and A.Nakazawa). Phages from positive plaques were purified to homogeneity and characterized using standard procedures (Steeghs *et al.*, 1997). Exons were identified using Southern blot hybridization with exon-specific oligonucleotides, and positioned by restriction mapping followed by partial sequence analysis of genomic DNA fragments. Appropriate segments that covered the entire exon 1–7 region of the AK1 gene were subcloned into plasmid pGEM3 (Promega). The 2.6 and 4.1 kb *Sal*I–*Bam*HI and *Hin*dIII–*Bam*HI fragments were used as left and right arms of homology to generate the targeting vector (Figure 1). In the construct, the exon 3–5 area, encoding the ATP binding site, was replaced by a *Bam*HI–*Hin*dIII hygromycin B resistance (hygroBʳ) cassette (van Deursen and Wieringa, 1992). To enable selection for homologous targeting, a negative selection cassette containing the 2.0 kb herpes simplex virus thymidine kinase gene (HSV-tk; van Deursen and Wieringa, 1992) was inserted at the 3′ *Bam*HI site. The AK1 targeting vector was linearized at the *Xba*I site located at the vector's multiple cloning site upstream of the 5′ AK1 insert.

AK1⁻/⁻ embryonic stem cells
Wild-type E14 ES cells were grown on a layer of irradiated SNLH9 feeder cells, cultured and electroporated (van Deursen and Wieringa, 1992; Steeghs *et al.*, 1997). Twenty-four hours after electroporation, cells were grown in the presence of 300 µg/ml hygromycin B (Life Technologies) and 0.2 µM Fiau (Bristol-Meyer), and allowed to grow for another 8–10 days before resistant colonies were isolated. For detection of the desired AK1 mutation, genomic DNAs from individual ES clones were prepared according to established procedures (Steeghs *et al.*, 1997). DNA was digested with either *Bam*HI or *Kpn*I–*Xho*I

restriction enzymes for the identification of targeted homologous recombination events at both sides of the replacement cassette (Steeghs *et al.*, 1997). The homologous recombination event at the 5′ side of the AK1 locus was determined using a unique 800 bp *Sal*I–*Kpn*I fragment as probe. For identification of the 3′ event, a 1700 bp *Bam*HI–*Xho*I fragment (Figure 1) was used.

AK1⁻/⁻ knockout mice
Targeted ES cells (AK1⁺/⁻) were injected into blastocysts derived from C57BL/6 mice to obtain chimeric, heterozygous and homozygous offspring (van Deursen *et al.*, 1993; Steeghs *et al.*, 1997). AK1⁻/⁻ mice were kept on a mixed 50%–50% C57BL/6 × 129/Ola inbred background during breeding. Southern analysis was performed on DNA from tail biopsies used for genotyping. A PCR assay was designed where three primers were used to discriminate between wild-type, heterozygous and homozygous mutant mice. Forward primer was AK1M1 located in intron 1 (5′-GGAGCCTGACACTTATTGCTG). Reverse primers were AK1M2 (5′-GAATTGCTGTCCGGTATAGC) and H1 (5′-GGCTGG-CACTCTGTCGATACCC) located in intron 2 and the hygromycin B resistance gene, respectively. PCR reactions were carried out in 50 ml containing 10 mM Tris–HCl pH 8.3, 50 mM KCl, 1.5 mM MgCl₂, 0.01% gelatin, 100 ng of each primer, 100 ng of DNA template and 1 U of *Taq* polymerase. Amplified products generated from the wild-type and AK1 mutant locus were 384 and 626 bp in length, respectively. GPS muscles from age-matched homozygous AK1-deficient and wild-type control animals, also having a 50%–50% C57BL/6 × 129/Ola mixed inbred background, were used throughout experiments. Under standard housing conditions, we saw no abnormalities in birth weight, weight gain during growth into adulthood, or daily food intake in first- and second-generation AK1⁻/⁻ animals. Also, fiber type distribution was normal in AK1 mice. Mice were anesthetized with 2,2,2-tribromoethanol (350 mg/kg i.p.) or pentobarbital (100 mg/kg i.p.). All procedures conformed to the *Guidelines for the Care and Use of Laboratory Animals* of the Dutch Council and the National Institutes of Health, and were approved by the Institutional Animal Care and Use Committee at the University of Nijmegen, the Mayo Clinic and the Vrije University, Amsterdam.

Northern blot analysis
Total RNAs from freshly isolated skeletal GPS muscle, as well as heart and brain, were extracted using the lithium chloride–urea method (Steeghs *et al.*, 1997) and analyzed by northern blotting (Steeghs *et al.*, 1997). RNA blots were hybridized with a fragment of rat AK1 cDNA, spanning exons 5–7, and a 1.3 kb rat glyceraldehyde-3-phosphate dehydrogenase (GAPDH) cDNA probe. Hybridization was carried out overnight at 65°C in 0.5 M NaPO₄ buffer pH 7.2, 7% (w/v) SDS, 1 mM EDTA, and blots were washed to a final stringency of 1× SSC/1% (w/v) SDS at 65°C and exposed on Kodak X-Omat films.

Zymogram analysis
Homogenates from freshly excised GPS muscles (10% w/v) were prepared in SETH buffer (250 mM sucrose, 2 mM EDTA, 10 mM Tris–HCl pH 7.4) at 4°C. GPS extracts were diluted 1:1 in 30 mM Na₃PO₄ buffer pH 7.4, containing 0.05% v/v Triton X-100, 0.3 mM dithiothreitol and a protease inhibitor cocktail (1 mM phenylmethylsul-fonyl fluoride, 10 µg/ml leupeptin, 1 µg/ml aprotinin; Boehringer Mannheim #1697498). Muscle extracts were incubated for 30 min at room temperature, centrifuged for 20 min at 11 000 *g* and an aliquot (1–5 µl) applied to agarose gels (Alameda, CA). AK1 and CK isoenzymes were separated electrophoretically, and stained for enzyme activity (Steeghs *et al.*, 1997).

Adenylate kinase and NDPK activity
AK activity was measured spectrophotometrically in GPS muscle extracts (Dzeja *et al.*, 1999). In addition, AK activity was measured by a luciferase-based ATP bioluminescence assay (Sigma) in the presence of 2 mM ADP using a BioOrbit 1253 luminometer. The NDPK activity, expressed in RLU/min/mg protein, was determined with the same bioluminescence assay in the presence of the AK inhibitor diadenosine pentaphosphate (Ap₅A; 200 µM), and the reaction started with dGTP (2 mM).

AMPD
AMPD activity was measured using GPS muscle extracts (Rush *et al.*, 1998). AMPD activity was measured in a reaction buffer containing 15 mM AMP, and formation of the reaction product, IMP, monitored by HPLC. Western blot analysis of AMPD was performed on muscle extracts probed with a polyclonal antiserum raised against purified rat

skeletal muscle AMPD. Developed nitrocellulose membranes were digitized and analyzed using NIH Image (Tullson *et al.*, 1998).

High-energy phosphoryl transfer

ATP turnover and phosphoryl flux through AK, CK and glycolytic systems were measured in intact GPS muscle complex using the [^{18}O]phosphoryl labeling technique (Zeleznikar and Goldberg, 1991; Zeleznikar *et al.*, 1995; Dzeja *et al.*, 1996, 1999). Isolated mouse GPS muscle was pre-incubated for 15–20 min at room temperature in media containing 137 mM NaCl, 5 mM KCl, 2 mM CaCl$_2$, 1 mM MgCl$_2$, 1 mM NaH$_2$PO$_4$, 20 mM HEPES, 0.05 mM EDTA, 5 mM glucose, 24 mM NaHCO$_3$ pH 7.4. The muscle complex was then rapidly transferred into media enriched with 20% [^{18}O]water (Isotec Inc.), and paced at 2 Hz. In separate experiments, hypoxia was simulated by pre-incubating muscles in 2 mM KCN for 3 min, and then transferring muscles into ^{18}O-enriched media with 2 mM KCN for an additional 3 min (at continuous 2 Hz pacing). Cellular ATP, ADP, GTP, GDP, inorganic phosphate, CrP and G-6-P were purified and quantified using high-performance liquid chromatography (HPLC) (Zeleznikar and Goldberg, 1991; Dzeja *et al.*, 1996). Samples containing phosphoryls of γ-ATP, β-ATP, β-ADP, γ-GTP, β-GTP, β-GDP, inorganic phosphate and CrP, as glycerol-3-phosphate, were converted to trimethylsilyl derivatives. ^{18}O enrichment of phosphoryls in glycerol-3-phosphates was determined with a Hewlett-Packard 5980B gas chromatograph mass spectrometer. Total cellular ATP turnover, along with net AK- and CK-catalyzed phosphotransfer, were determined from the rate of appearance of ^{18}O-containing phosphoryls (Zeleznikar *et al.*, 1990; Zeleznikar and Goldberg, 1991; Dzeja *et al.*, 1996). The rate of net phosphoryl flux through the glycolytic system was measured by the appearance of ^{18}O-labeled phosphoryls in G-6-P, which was purified by HPLC (Dzeja *et al.*, 1996).

Metabolite levels

ATP, ADP, AMP, GTP and GDP levels were quantified in perchloric muscle extracts by HPLC (Zeleznikar and Goldberg, 1991; Dzeja *et al.*, 1999). CrP, muscle lactate and G-6-P levels were determined using coupled enzyme assays (van Deursen *et al.*, 1993; Dzeja *et al.*, 1996). Muscle inorganic phosphate level was determined using the EnzChek Phosphate Assay kit (Molecular Probes).

In vivo ^{31}P-NMR spectroscopy

In mice anesthetized with 1.5% enflurane, ^{31}P-NMR spectra were determined *in vivo* in hind limb muscles using a 7T S.M.I.S. spectrometer. Recordings were performed prior to, during 25 min of ischemia and following 16 min of reperfusion. Ischemia was induced by occluding hind limb circulation. Spectra were analyzed using time domain fitting, and normalized to the mean value of the β-ATP intensity of the first four spectra.

Contractile muscle properties

Peak force, maximal rate of force rise and half-relaxation time were obtained under isometric conditions in medial gastrocnemius muscles (at 35°C) from wild-type and AK1-deficient mice (*n* = 20) as described (de Haan *et al.*, 1989). Maximal shortening velocity was obtained in a subgroup by extrapolation of the force–velocity relationship. Fatigability was investigated by applying a series of 20 isometric contractions (150 ms duration, 150 Hz) within 10 s.

Statistics

Data are presented as mean ± SE, unless indicated otherwise. Student's *t*-test for unpaired samples was used for statistical analysis, and $p < 0.05$ was considered significant.

Acknowledgements

References

Bandlow,W., Strobel,G., Zoglowek,C., Oechsner,U. and Magdolen,V. (1988) Yeast adenylate kinase is active simultaneously in mitochondria and cytoplasm and is required for non-fermentative growth. *Eur. J. Biochem.*, **178**, 451–457.

Bessman,S.P. and Carpenter,C.L. (1985) The creatine–creatine phosphate energy shuttle. *Annu. Rev. Biochem.*, **54**, 831–862.

Collavin,L., Lazarevic,D., Utrera,R., Marzinotto,S., Monte,M. and Schneider,C. (1999) wt p53 dependent expression of a membrane-associated isoform of adenylate kinase. *Oncogene*, **18**, 5879–5888.

de Haan,A., Jones,D.A. and Sargeant,A.J. (1989) Changes in velocity of shortening, power output and relaxation rate during fatigue of rat medial gastrocnemius muscle. *Pflugers Arch.*, **413**, 422–428.

Dzeja,P.P. and Terzic,A. (1998) Phosphotransfer reactions in the regulation of ATP-sensitive K$^+$ channels. *FASEB J.*, **12**, 523–529.

Dzeja,P.P., Zeleznikar,R.J. and Goldberg,N.D. (1996) Suppression of creatine kinase-catalyzed phosphotransfer results in increased phosphoryl transfer by adenylate kinase in intact skeletal muscle. *J. Biol. Chem.*, **271**, 12847–12851.

Dzeja,P.P., Zeleznikar,R.J. and Goldberg,N.D. (1998) Adenylate kinase: kinetic behavior in intact cells indicates it is integral to multiple cellular processes. *Mol. Cell. Biochem.*, **184**, 169–182.

Dzeja,P.P., Vitkevicius,K.T., Redfield,M.M., Burnett,J.C. and Terzic,A. (1999) Adenylate kinase-catalyzed phosphotransfer in the myocardium: increased contribution in heart failure. *Circ. Res.*, **84**, 1137–1143.

Dzeja,P.P., Redfield,M.M., Burnett,J.C. and Terzic,A. (2000) Failing energetics in failing hearts. *Curr. Cardiol. Rep.*, **2**, 212–217.

Elvir Mairena,J.R., Jovanovic,A., Gomez,L.A., Alekseev,A.E. and Terzic,A. (1996) Reversal of the ATP-liganded state of ATP-sensitive K$^+$ channels by adenylate kinase activity. *J. Biol. Chem.*, **271**, 31903–31908.

Gibbs,C.L. and Barclay,C.J. (1998) Efficiency of skeletal and cardiac muscle. *Adv. Exp. Med. Biol.*, **453**, 527–536.

Hardie,D.G. and Carling,D. (1997) The AMP-activated protein kinase fuel gauge of the mammalian cell? *Eur. J. Biochem.*, **246**, 259–273.

Kay,L., Nicolay,K., Wieringa,B., Saks,V. and Wallimann,T. (2000) Direct evidence for the control of mitochondrial respiration by mitochondrial creatine kinase in oxidative muscle cells *in situ*. *J. Biol. Chem.*, **275**, 6937–6944.

Konrad,M. (1993) Molecular analysis of the essential gene for adenylate kinase from the fission yeast *Schizosaccharomyces pombe*. *J. Biol. Chem.*, **268**, 11326–11334.

Koretsky,A.P. (1995) Insights into cellular energy metabolism from transgenic mice. *Physiol. Rev.*, **75**, 667–688.

Lu,Q. and Inouye,M. (1996) Adenylate kinase complements nucleoside diphosphate kinase deficiency in nucleotide metabolism. *Proc. Natl Acad. Sci. USA*, **93**, 5720–5725.

Matsuura,S. *et al.* (1989) Human adenylate kinase deficiency associated with hemolytic anemia. A single base substitution affecting solubility and catalytic activity of the cytosolic adenylate kinase. *J. Biol. Chem.*, **264**, 10148–10155.

Mommaerts,W.F. (1969) Energetics of muscular contraction. *Physiol. Rev.*, **49**, 427–508.

Nobumoto,M., Yamada,M., Song,S., Inouye,S. and Nakazawa,A. (1998) Mechanism of mitochondrial import of adenylate kinase isozymes. *J. Biochem.*, **123**, 128–135.

Noda,L.H. (1973) Adenylate kinase. In Boyer,P.D. (ed.), *The Enzymes*. Vol. VIII. Academic Press, New York, NY, pp. 279–305.

Olson,L.K., Schroeder,W., Robertson,R.P., Goldberg,N.D. and Walseth,T.F. (1996) Suppression of adenylate kinase catalyzed phosphotransfer precedes and is associated with glucose-induced insulin secretion in intact HIT-T15 cells. *J. Biol. Chem.*, **271**, 16544–16552.

Ottaway,J.H. and Mowbray,J. (1977) The role of compartmentation in the control of glycolysis. *Curr. Top. Cell. Regul.*, **12**, 107–208.

Ray,N.B. and Mathews,C.K. (1992) Nucleoside diphosphokinase: a functional link between intermediary metabolism and nucleic acid synthesis. *Curr. Top. Cell. Regul.*, **33**, 343–357.

Rush,J.W., Tullson,P.C. and Terjung,R.L. (1998) Molecular and kinetic alterations of muscle AMP deaminase during chronic creatine depletion. *Am. J. Physiol.*, **274**, C465–C471.

Saks,V., Dos Santos,P., Gellerich,F.N. and Diolez,P. (1998) Quantitative studies of enzyme substrate compartmentation, functional coupling and metabolic channelling in muscle cells. *Mol. Cell. Biochem.*, **184**, 291–307.

Saupe,K.W., Spindler,M., Tian,R. and Ingwall,J.S. (1998) Impaired cardiac energetics in mice lacking muscle-specific isoenzymes of creatine kinase. *Circ. Res.*, **82**, 898–907.

Savabi,F. (1994) Interaction of creatine kinase and adenylate kinase systems in muscle cells. *Mol. Cell. Biochem.*, **133–134**, 145–152.

Schulz,G.E., Schiltz,E., Tomasselli,A.G., Frank,R., Brune,M., Wittinghofer,A. and Schirmer,R.H. (1986) Structural relationships in the adenylate kinase family. *Eur. J. Biochem.*, **161**, 127–132.

Steeghs,K. *et al.* (1997) Altered Ca^{2+} responses in muscles with combined mitochondrial and cytosolic creatine kinase deficiencies. *Cell*, **89**, 93–103.

Steeghs,K. *et al.* (1998) Cytoarchitectural and metabolic adaptations in muscles with mitochondrial and cytosolic creatine kinase deficiencies. *Mol. Cell. Biochem.*, **184**, 183–194.

Tanabe,T., Yamada,M., Noma,T., Kajii,T. and Nakazawa,A. (1993) Tissue-specific and developmentally regulated expression of the genes encoding adenylate kinase isozymes. *J. Biochem.*, **113**, 200–207.

Tullson,P.C. and Terjung,R.L. (1991) Adenine nucleotide metabolism in contracting skeletal muscle. *Exerc. Sport Sci. Rev.*, **19**, 507–537.

Tullson,P.C., Rush,J.W., Wieringa,B. and Terjung,R.L. (1998) Alterations in AMP deaminase activity and kinetics in skeletal muscle of creatine kinase-deficient mice. *Am. J. Physiol.*, **274**, C1411–C1416.

van Deursen,J. and Wieringa,B. (1992) Targeting of the creatine kinase M gene in embryonic stem cells using isogenic and nonisogenic vectors. *Nucleic Acids Res.*, **20**, 3815–3820.

van Deursen,J., Heerschap,A., Oerlemans,F., Ruitenbeek,W., Jap,P., ter Laak,H. and Wieringa,B. (1993) Skeletal muscles of mice deficient in muscle creatine kinase lack burst activity. *Cell*, **74**, 621–631.

Veksler,V.I., Kuznetsov,A.V., Anflous,K., Mateo,P., van Deursen,J., Wieringa,B. and Ventura Clapier,R. (1995) Muscle creatine kinase-deficient mice. II. Cardiac and skeletal muscles exhibit tissue-specific adaptation of the mitochondrial function. *J. Biol. Chem.*, **270**, 19921–19929.

Wallimann,T., Wyss,M., Brdiczka,D., Nicolay,K. and Eppenberger,H.M. (1992) Intracellular compartmentation, structure and function of creatine kinase isoenzymes in tissues with high and fluctuating energy demands: the 'phosphocreatine circuit' for cellular energy homeostasis. *Biochem. J.*, **281**, 21–40.

Wegmann,G., Zanolla,E., Eppenberger,H.M. and Wallimann,T. (1992) *In situ* compartmentation of creatine kinase in intact sarcomeric muscle: the acto-myosin overlap zone as a molecular sieve. *J. Muscle Res. Cell Motil.*, **13**, 420–435.

Yan,H. and Tsai,M.D. (1999) Nucleoside monophosphate kinases: structure, mechanism, and substrate specificity. *Adv. Enzymol. Relat. Areas Mol. Biol.*, **73**, 103–134.

Zeleznikar,R.J. and Goldberg,N.D. (1991) Kinetics and compartmentation of energy metabolism in intact skeletal muscle determined from ^{18}O labeling of metabolite phosphoryls. *J. Biol. Chem.*, **266**, 15110–15119.

Zeleznikar,R.J., Heyman,R.A., Graeff,R.M., Walseth,T.F., Dawis,S.M., Butz,E.A. and Goldberg,N.D. (1990) Evidence for compartmentalized adenylate kinase catalysis serving a high energy phosphoryl transfer function in rat skeletal muscle. *J. Biol. Chem.*, **265**, 300–311.

Zeleznikar,R.J., Dzeja,P.P. and Goldberg,N.D. (1995) Adenylate kinase-catalyzed phosphoryl transfer couples ATP utilization with its generation by glycolysis in intact muscle. *J. Biol. Chem.*, **270**, 7311–7319.